JOURNAL OF SPACECRAFT AND ROCKETS
Vol. 39, No. 2, March–April 2002

Electric Propulsion Space Experiment (ESEX) On-Orbit Results

D. R. Bromaghim,* J. R. LeDuc,† R. M. Salasovich,† G. G. Spanjers,† J. M. Fife,†
M. J. Dulligan,‡ J. H. Schilling,§ and D. C. White§
U.S. Air Force Research Laboratory, Edwards Air Force Base, California 93524-7013
and
L. K. Johnson¶
The Aerospace Corporation, El Segundo, California 90245

The U.S. Air Force Research Laboratory's Electric Propulsion Space Experiment was launched and successfully operated, demonstrating the compatibility and readiness of a 26-kW ammonia arcjet subsystem for satellite applications. The Electric Propulsion Space Experiment is one of nine experiments on the U.S. Air Force's Advanced Research and Global Observation Satellite. Data were acquired to characterize the thruster in four different areas: electromagnetic interactions, contamination effects, optical properties of the plume, and thruster system performance. The results demonstrated that the critical system components including the arcjet, power processor, and propellant system operated well and verified the interoperability of high-power electric propulsion with generic satellite operations.

Introduction

THE Electric Propulsion Space Experiment (ESEX) was a space demonstration of a 26-kW ammonia arcjet sponsored by the U.S. Air Force Research Laboratory with TRW, Inc., as the prime contractor. The experiment objectives were to demonstrate the feasibility and compatibility of a high-power arcjet system, as well as measure and record flight data for comparison to ground results.[1–3] The onboard flight diagnostics included four thermoelectrically cooled quartz crystal microbalance (TQCM) sensors, four radiometers, a section of eight gallium–arsenide (Ga–As) solar array cells, electromagnetic interference (EMI) antennas, a video camera, and an accelerometer. ESEX was one of nine experiments on the Advanced Research and Global Observation Satellite (ARGOS), launched on 23 February 1999 from Vandenberg Air Force Base, California, on a Delta II into a nominal orbit of approximately 846 km at 98.7-deg inclination.[4,5] Once on-orbit, the satellite was operated from the research, development, test, and evaluation support complex at the Space and Missile Test and Evaluation Directorate at Kirtland Air Force Base, New Mexico.

The ESEX flight system (Fig. 1) includes a propellant feed system (PFS),[6] power subsystem[7] including the power conditioning unit (PCU)[8] and the silver–zinc battery, commanding and telemetry modules, the onboard diagnostics,[1] and the arcjet assembly.[8] ESEX was designed and built as a self-contained experiment to minimize the impact of any effects from the arcjet firings on ARGOS. This design allowed ESEX to function semi-autonomously, requiring ARGOS support only for attitude control, communications, radiation-hardened data storage, and housekeeping power for functions such as battery charging and thermal control.

Received 19 January 2001; revision received 13 August 2001; accepted for publication 13 August 2001.

*Program Manager, Propulsion Directorate, AFRL/PRSS. Member AIAA.
†Project Engineer/Scientist, Propulsion Directorate, AFRL/PRSS. Member AIAA.
‡Project Scientist, ERC, Inc. Member AIAA.
§Project Scientist, Sparta, Inc.; currently Project Scientist, W.E. Research, 4360 San Juan Court, Rosamond, CA 93560. Member AIAA.
¶Electric Propulsion Space Experiment Chief Scientist; currently Research Scientist, Thermal and Propulsion Engineering Department, Jet Propulsion Laboratory, MS 125-109, California Institute of Technology, 4800 Oak Grove Drive, Pasadena, CA 91109.

The ESEX flight operations focused on scheduling firings concurrent with observable passes over ground-based sensors in northern California and Maui, Hawaii. The eight firings were executed mostly without incident, and the arcjet, PCU, and PFS performed well. Ultimately, however, a battery anomaly occurred that precluded further firings.

Data from all of the onboard diagnostics were collected for each firing. Ground-based measurements were performed for several of the firings as well. In general, the performance of the thruster was nominal and, although there were measurable effects observed, none of the onboard or remote diagnostics indicated any issues with integrating high-power electric propulsion onto spacecraft. Furthermore, none of the firings showed any negative effect on the ARGOS operations.

This paper describes the flight operations, followed by a summary of the science data results, and concludes with a discussion of the two anomalies experienced during the mission. Companion papers discuss the design and development of the arcjet, PCU, and associated hardware, the integration and test activities, and the science results in detail.[9–17]

Flight Operations Overview

Prelaunch Activities

After a substantial test and evaluation program of the ARGOS spacecraft,[18] the satellite, with ESEX integrated, was shipped to Vandenberg Air Force Base for launch. After a functional verification was performed, ARGOS was mated to the Delta II to complete the final launch preparations. A series of tests were conducted while the vehicle was in this configuration including several functional verification tests, ESEX and ARGOS battery maintenance, and a communications compatibility verification with the Air Force Satellite Control Network (AFSCN).

Launch Attempts

There were a total of 10 scrubbed launch attempts, the bulk of which resulted from inclement weather. The weather violations were dominated by winds aloft that either exceeded the maximum loading requirements on the Delta II fairing, or that would have created a potential hazard for falling debris on populated areas. The vehicle was ultimately launched successfully on 23 February 1999. The Delta II placed ARGOS within 1% of the nominal sun synchronous orbit at an altitude of 846.2 km, and an inclination of 98.73 deg, corresponding to an orbital period of 101.6 min.

Phase I Operations

After the successful launch and initial acquisition and stabilization, the operations focused on verifying the spacecraft bus and all of

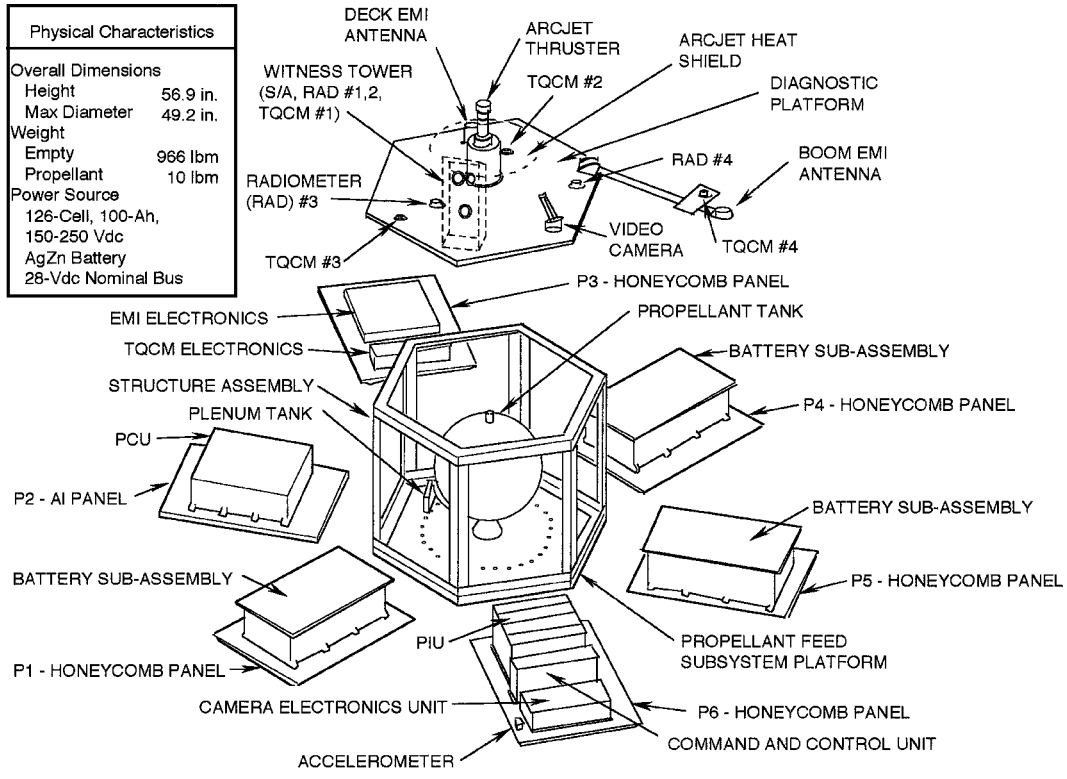

Fig. 1 Exploded view of the ESEX flight unit.

the experiments, including ESEX, were fully operational. ARGOS completed the nominal initialization process except for two issues. The first was a propensity of the global positioning system (GPS) receiver to drop out of the navigation mode, the method by which a position and velocity solution are determined. This behavior was eventually traced to a signal-to-noise problem, but eliminated the planned use of the receiver by ESEX as one technique to measure arcjet performance.[3] This problem was partially resolved after the ESEX operations were complete by uploading a software patch to the ARGOS flight computer.

The second issue was a recurrence of a ground-test anomaly, which was manifested as an inability to perform ranging, commanding, and telemetry downlink simultaneously with the AFSCN standard uplink power and command modulation index. The issue was mostly eliminated early in phase I by modifying the standard uplink power and command modulation index at each AFSCN site, until a satisfactory communications link was established. The problem did appear periodically throughout the remainder of the ESEX mission, however, and hampered some of the electromagnetic test objectives.

On day 2, approximately 26 h after launch, the vehicle received an incorrect GPS initialization vector and went into the spacecraft safe mode, known as sunsafe, that inertially points the arrays at the sun and turns off all unnecessary power loads. This configuration optimizes the chances of survival given an anomaly of unknown origin. The cause here, however, was a known problem (an incorrect initialization vector), and the recovery process was started immediately.

Phase I continued approximately 48 h later, and at that time the first of two ESEX anomalies were observed. As a part of the power reduction procedure executed when ARGOS enters sunsafe mode, a series of lower heater setpoints are triggered for several ESEX components including the battery panels, which have thermostatically controlled bleed resistors designed to dissipate the battery charge following the end of phase II. These resistors were engaged as a result of all sunsafe events, requiring battery charging immediately following the completion of the sunsafe recovery. During the first of these charging cycles, high oscillations on the battery charger output were observed when the battery voltage reached −225 V dc. This behavior, and the impact to the ESEX mission, is discussed in a later section on flight anomalies.

After verifying that the anomalous charger–circuit behavior was not detrimental to the flight unit, the ESEX battery charging was continued. The remainder of the ESEX initialization and checkout was completed, which included a verification of all of the electronic boxes, the thermal control system, and the command sequences used to control the majority of the ESEX operations.[18] The ESEX EMI boom was deployed on day 14, later than originally planned.[18] The deployment was delayed to allow additional outgassing data to be collected from TQCM sensor 4, located on the EMI boom, while it was pointed at the ESEX diagnostic deck in the stowed position. Once the initialization activities were successfully completed, ESEX and ARGOS were declared ready to support experiment operations, and phase II began.

Phase II Operations

Phase II was dedicated to two primary experiments[4,5]: ESEX and the critical ionization velocity (CIV)[4] experiment. The original operations plan called for integrating ESEX firings with CIV releases for the duration of the mission. This plan did not prove logistically feasible on-orbit due to a shorter amount of time between ESEX firings than planned, coupled with weather and instrument problems at the ground observation sites. The modified experimental plan did not significantly affect either the CIV or ESEX mission success.

The first ESEX activity in phase II was to perform a series of outflows from the PFS, first with nitrogen followed by ammonia, while monitoring the ESEX and ARGOS state of health telemetry. These activities are summarized in Table 1. The objective of these outflows was fourfold: 1) to bleed the nitrogen blanket from the plenum tank, 2) to verify the operation of the PFS, 3) to verify that the arcjet cold flow thrust would not have a detrimental effect on the ARGOS attitude control system, and 4) to measure any off-axis thrust (which there was none). The nitrogen outflow was performed by opening the arcjet valve without activating the PFS algorithm, the software method by which flow to the arcjet is actively controlled.[9] The outflow was conducted over two passes, to allow enough time to evacuate the plenum tank pressure to <7000 Pa. The ammonia release was planned in the same pass as the second nitrogen release (R-2), but was aborted by the ESEX computer when an overly conservative, self-imposed software limit on the PFS temperature was exceeded. This temperature limit is one of several ESEX inputs that

Table 1 Summary of ESEX arcjet firings and propellant releases

Firing (F) or release (R)	Date/time	Duration, min:s (s)	Location	Comments
R-1 (N_2)	11 March 1999, 1928 Z	8:29 (509)	Not observed	Initial N_2 bleed required majority of pass.
R-2 (N_2/NH_3)	12 March 1999, 0027 Z	1:13 (73)	Not observed	N_2 bleed completed. NH_3 aborted due to overly conservative software constraints on PFS heaters.
R-3 (N_2/NH_3)	12 March 1999, 1258 Z	1:59/3:59 (119/239)	Not observed	All systems operated nominally. Liquid ingestion first observed.
F-1A	13 March 1999, 1240 Z	N/A	MSSS	First arcjet ignition (on 10th start pulse), firing aborted due to overly conservative sofware constraints on mass flow rate.
F-1B	15 March 1999, 1210 Z	N/A	MSSS	Firing attempt aborted due to overly conservative software constraints on PFS heaters.
F-1C	15 March 1999, 2155 Z	2:21 (141)	CPCA	Modified firing sequence to account for liquid ingestion and ensure vapor outflow to arcjet. CPCA performed passive data collection.
F-2	19 March 1999, 2232 Z	5:01 (301)	CPCA	Flow rate setpoint increased to 250 mg/s. All systems operated nominally. CPCA acquired first active data set.
F-3	21 March 1999, 1224 Z	5:33 (333)	MSSS	All systems operated nominally. No MSSS data acquired due to inclement weather.
F-4	23 March 1999, 2127 Z	8:02 (482)	CPCA	All systems operated nominally except for low battery output voltage, caused arcjet to shut off early. First indication of battery trouble.
F-5	26 March 1999, 2145 Z	6:04 (364)	MSSS	Low battery voltage forced early termination. Telemetry dropouts observed. MSSS acquired first space-based arcjet firing spectra.
R-4 (NH_3)	30 March 1999, 0636 Z	8:54 (534)	N/A	Attempted PFS heater modifications to eliminate liquid ingestion do not succeed.
F-6	31 March 1999, 1305 Z	4:30 (270)	MSSS	Low battery voltage forced early termination. Telemetry dropouts reduced by increased ground transmitter power. No firing spectra acquired.
F-7A/B	2 April 1999, 2209 Z	53 s/38 s	CPCA	Attempt to discharge battery as much as possible before reconditioning. Arcjet stopped/restarted due to PCU command logic. CPCA acquired start and stop transient data.
R-5 (NH_3)	9 April 1999, 1548 Z	9:06 (546)	N/A	Further attempts to eliminate liquid ingestion with PFS heater modifications proved unsuccessful.
F-8	21 April 1999, 1222 Z	42 s	MSSS	Battery reconditioning had no effect. No MSSS data acquired. No liquid ingestion observed.

allow the operator to establish control parameters within which the ESEX computer must function. The ESEX computer compares the measured value with the user-established limit 30 times/s, and it aborts all operations and safes the system if the measured value violates the limit. For the R-2 release attempt, the baseline limits, which were preprogrammed before launch, were too constraining. This overconservatism was somewhat expected because the preprogrammed limits represented the designers' best estimate of the on-orbit conditions. The second release attempt (R-3) was executed successfully with a more relaxed but acceptable limit and exhibited nominal behavior except for a momentary ingestion of a slug of liquid ammonia at the initialization of the PFS algorithm. The ingestion was overcome by implementing an operational delay after opening the arcjet valve, which allowed the plenum tank to dry out and the flow to stabilize before starting the arcjet. This is discussed in detail in a later section on flight anomalies.

The duty cycle of the flow control valve, the dual pressure control (DPC) valve, showed a large control margin. In fact, the measured flow rate was often within ± 0.3 mg/s of the setpoint, well within the specified requirement of ± 5 mg/s.

Once the PFS operation was verified, the arcjet firings were initiated. The firings were all conducted over two ground sites to facilitate ground-based observations.[3,19] The two sites used were the 1.6-m telescope at the Maui Space Surveillance Site (MSSS) for optical observations[12] and the Camp Parks Communications Annex (CPCA) in Dublin, California, for the communication experiments.[13] A brief summary of all of the arcjet firings is included in Table 1.

The first two firing attempts (F-1A and F-1B) were aborted due to overly conservative software constraints, similar to the experience on the first ammonia outflow. These initial adjustments to the ESEX system were not unexpected and did not reflect system behavior that was anomalous or out of specification. Subsequent data review showed the arcjet actually ignited on the first firing attempt (F-1A) on the 10th start pulse, but was aborted within 2–3 s due to a mass flow rate limit that was too tight for the ramp-up phase. The second firing attempt (F-1B) was aborted by a temperature software limit before the arcjet start command.

The need for 10 start pulses to ignite the thruster on the first attempt is consistent with ground-test experience, where multiple start pulses were often used. Additionally, flight experience with other arcjets has typically shown the first on-orbit ignition to be slightly more difficult than all subsequent starts, possibly due to oxidation or slight, unavoidable contamination of the cathode from ground handling, cleanliness levels, etc. Interestingly, all subsequent firings ignited on the first pulse, validating the work done early in the program to ensure reliable arcjet starts.[20–22] The first successful arcjet firing (F-1C) was completed after a thorough review of all software limits. The planned duration for the first firing was 4 min (Refs. 18 and 19) but was terminated after 141 s because the contact support for that orbit pass was ending, mostly as a result of the delay from the liquid ingestion. This firing was performed over CPCA, which passively acquired data on the ARGOS transmission spectra. The results acquired from CPCA are discussed briefly here and detailed by Dulligan et al.[13]

Subsequent firings proceeded much in the same manner as firing F-1C. The mass flow rate for the remaining firings was increased, however, because the arcjet power appeared higher than the nominal 26 kW. Later analyses indicated the higher power readings may have been erroneous, as discussed in detail by Fife et al.[14] Figure 2 shows a typical operational data set for a firing, in this case from firing F-4 on 23 March 1999. As shown in Fig. 2, all of the demonstration components (the arcjet, PCU, and PFS) operated well, typically well within the specifications set forth at program initiation. The liquid ingestion can be seen in Fig. 2, as well as a drop in the battery output voltage indicative of the deteriorating battery state of health. The low battery voltage ultimately caused the arcjet to shut off because it was below the acceptable PCU input voltage.

Battery charging was conducted between each of the firings, which, as described earlier, were scheduled on high-elevation passes at either MSSS or CPCA. This scheduling philosophy maximized the opportunities to collect data from the ground-based observations, but limited the duration of each firing by limiting the amount of charging between each event.

Phase II proceeded with seven more ESEX firings and the CIV releases. The ESEX flight unit performed flawlessly, in spite of minor issues with the PFS liquid ingestion, battery voltage fluctuations, and some telemetry issues with the arcjet current and inlet pressure. Each of the issues was ameliorated with relatively simple operational work-around procedures and had no detrimental effects on

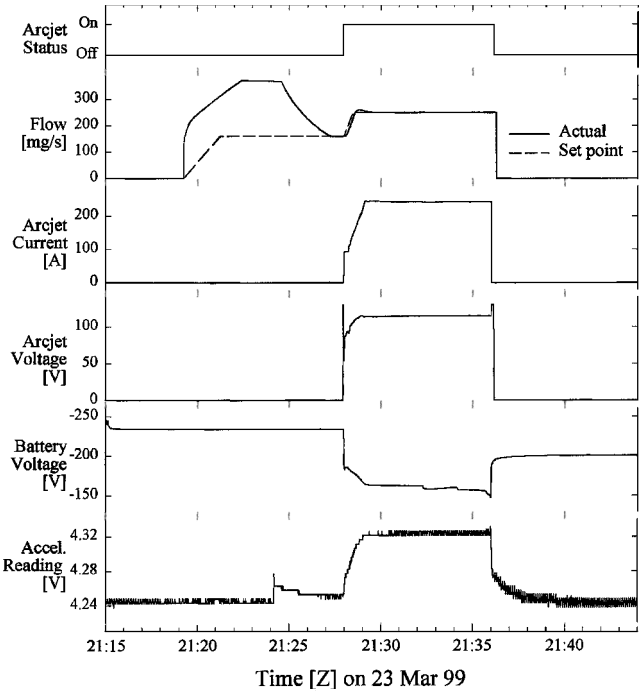

Fig. 2 Typical operational profile of an arcjet firing showing the ramp to full power and steady-state operation.

the ESEX or ARGOS system performance. Ultimately, however, the battery failed completely, eliminating any chance of further ESEX firings. Because this failure occurred within days of the scheduled end of phase II and the majority of science data had been collected, the result was only a minor impact on the overall mission success. Once the battery condition was stabilized, ESEX was placed into a long-term discharge configuration for the phase III portion of the ARGOS mission. The battery discharge was completed in July 1999, but the flight unit power remained on until August 2000 while contamination and electromagnetic data continued to be collected.

Science Results Summary

Although the mission was shortened somewhat by the battery failure, there was still an enormous amount of data collected during this unique opportunity. The science data were divided into four areas corresponding to the scientific objectives and the specific sensors.[3,19] These areas are optical observations, electromagnetic interactions, performance, and contamination measurements.[11–17]

Optical Observations

Optical observations were made from a ground-based sensor, the 1.6-m telescope/spectrograph at the MSSS observatory on Maui, Hawaii, as well as by an onboard still charge-coupled device (CCD) camera. The objective of these observations was to characterize the emitting excited states both from a spectroscopic and spatial perspective. Emission more than a few millimeters from the nozzle arises from recombination, and consequently the measurement environment is expected to be significant to the observations. The ESEX flight was the first opportunity to observe a high-power plume expansion under molecular flow conditions inasmuch as ground emission measurements have all been performed at considerably higher background pressure.

Spectroscopic data were expected to yield information about the energy distribution of excited states and, thus, contribute to the overall understanding of losses in the arcjet. The spectroscopic data were also expected to include continuum emission from the hot arcjet nozzle. These graybody temperature data could then be compared to nozzle temperatures measured in ground tests. Specifically, the primary intent of these observations was to closely examine the NH $(A–X)$ transition at moderately high resolution in an effort to determine vibrational and rotational temperatures in the plume. Unfortunately, a very small subset of the anticipated ground-based spectroscopic data was obtained during the flight campaign. Only a single observed firing provided useful data and recorded arcjet emission over the spectral range 320–670 nm at low resolution. In addition, poor weather conditions during the observed pass made unambiguous spectral intensity calibration difficult, and unfortunately the spectral resolution is not high enough to make reasonable estimates of the NH temperatures.

In spite of the difficulties, data from the single observed firing were examined and do provide some qualitative insight into the on-orbit arcjet firings. The principal features observed from the flight agree with ground tests[12]; namely, atomic hydrogen lines corresponding to the hydrogen Balmer series dominate the spectrum, along with the NH complex at near-UV wavelengths. As expected, the emission lines also sit on top of a graybody continuum rising to the red end of the spectrum. An analysis was performed to scale the continuum radiation to a blackbody energy distribution to estimate the temperature of the nozzle. The best curve fit corresponds to a temperature of 1840 ± 40 K, somewhat less than the peak temperature of 2100 K at the nozzle end measured on the ground. The discrepancy can be attributed to several considerations. First, relatively cooler as well as the hottest parts of the nozzle contribute to the on-orbit measurement of the continuum radiation, which reduces the overall measured temperature, whereas the ground-test measurement was made at the hottest part of the nozzle using an optical pyrometer with a spot size considerably smaller than the diameter of the nozzle. In addition, the flight observation was made after approximately 5 min of firing, whereas the ground observations were performed toward the end of a 15-min firing. The longer firing time presumably would present higher temperatures because the thruster heats during firing. Finally, differences in the thruster thermal environment, specifically the lower starting temperature in space and the presence of a room-temperature chamber radiating to the thruster in the ground test, would be expected to make the ground-test results hotter.

The video camera provided a verification of normal arcjet operation and was partly intended as a diagnostic for anomalous operation. More important, however, was the expectation that the video images would reveal the extent of the emitting part of the plume to be smaller than that observed on the ground because a small recombination volume is expected in space. Finally, the images were expected to confirm temporal and spatial aspects of arcjet nozzle heating models.

The onboard camera acquired images during each of the eight firings with several different shutter speed settings. The limited number of arcjet firings precluded testing over the full dynamic range of the camera, leading to the majority of the full-power images exceeding the maximum intensity range of the CCD detector. A survey of images of the arcjet during the first 90 s of operation illustrates the rapid heating of the anode and extent of the plume. Part of this series is shown in Fig. 3, which shows the startup and most of the 70-s ramp to full power. The lack of steady-state images precluded quantitative correlation of arcjet thermal models to the on-orbit data,

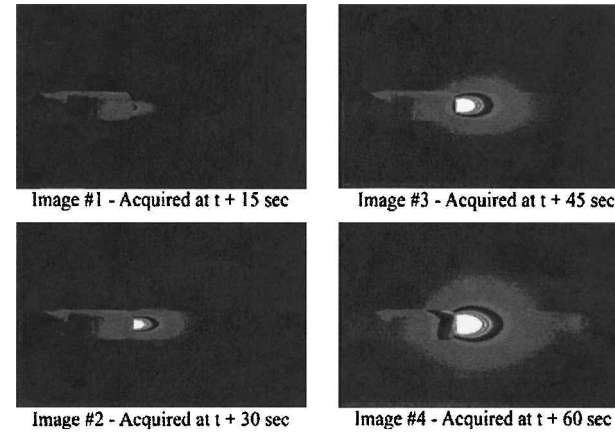

Fig. 3 Series of images acquired from the onboard video camera showing the ramp to full power ($t = 0$ is the time the arcjet was started).

but the results did qualitatively confirm the expectation of a smaller plume. These images confirmed the expectation that test chamber walls can affect ground-based measurements of high-power electric propulsion devices because plume expansion will be limited by the facility size and pumping capability.

Electromagnetic Interactions

The impacts of a 26-kW arcjet on spacecraft communications and operations have always been a major integration concern. A series of tests were performed during the ESEX mission to address as many of these areas as possible. Tests included measurements from the onboard EMI antennas, communication bit error rate (BER) tests to quantify the effect of the arcjet on the ranging signal, and uplink/downlink tests to verify qualitatively the communication link integrity. The results from the uplink/downlink test, and other qualitative results from the performance of the ARGOS subsystems, all indicate the arcjet firings had no deleterious effect on the ARGOS operations.[13]

The onboard EMI antennas measured the radiated emission from the arcjet in the lower gigahertz communication frequencies, for example, S-band, X-band, etc. The antennas sample 2-, 4-, 8-, and 12-GHz signals with a ±5% bandpass filter on each channel. Data were gathered on the antennas for each of the firings, during quiescent spacecraft periods and during routine spacecraft operations. The firing and nonfiring data sets were then compared to identify any effects from the arcjet operation. The antenna measurements during arcjet firing periods did not differ from nonfiring data and correspond well with measurements made during ground tests.[23]

The BER test enabled a quantified assessment of the effect of the arcjet on the satellite ranging channel. This test is performed by replacing the normal ranging pattern with a test pattern from CPCA and determining the number of bit errors on the return signal using a BER counter.[3,13,19] A series of baseline measurements were made while the arcjet was off and with the vehicle in several transmit configurations for comparison with firing data. Figure 4 shows the composite of all of the firing data compared with the baseline data acquired while the arcjet was not operating. These data were recorded at transmit rates of 1.024×10^6 bps, with typical error rates less than 2 bits in 10,000. Note that the CPCA system was significantly detuned by reducing the transmit power and adjusting the modulation index until a BER of 10 in 1×10^6 bits was typically observed at the minimum satellite range. During routine satellite operations, for instance, the BER is typically less than 1 in 1×10^6 bits. This detuning increased the sensitivity of the measurements to a point whereby even the smallest effects from the arcjet firings could be observed. If the data had shown an effect, the power and modulation index would have been adjusted until a more typical BER was observed and those results published for operational use.

In total, 3 arcjet firings and over 30 baseline BER curves were recorded during the ESEX flight. Analyses did not reveal a clear correlation between features observed in the arcjet firing curves and the operation of the arcjet because similar features are identifiable in both baseline and arcjet firing curves.

Performance

The arcjet performance was measured by three different techniques: an onboard accelerometer, AFSCN tracking, and the ARGOS GPS receiver.[14] Although there were some issues with both the accelerometer and the GPS data as described next, the ΔV derived from each of these techniques agree to within 1%. This correlation suggests that these data accurately represent the thruster performance.

The onboard accelerometer data were collected for all eight firings. There are a number of uncertainties in the thrust derived from the acceleration measurement, dominated by the systematic uncertainties associated with the accelerometer, PFS, and PCU. Figure 5 shows the mean specific impulse I_{sp} for the firings as a filled diamond plotted against the ground-test data on the engineering model hardware (shown as ×s in Fig. 5), along with a set of diagonal lines that correspond to a regression fit of previous performance data on a similar laboratory model ammonia arcjet.[24] Although the flight data agree with the performance measured during ground tests within the uncertainty of the measurement, the results were lower than expected. Following an investigation into the discrepancy, data

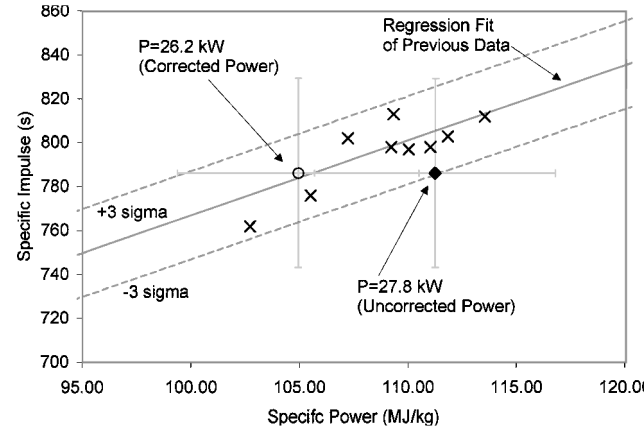

Fig. 5 Summary of the arcjet on-orbit mean performance showing the corrected and uncorrected results.

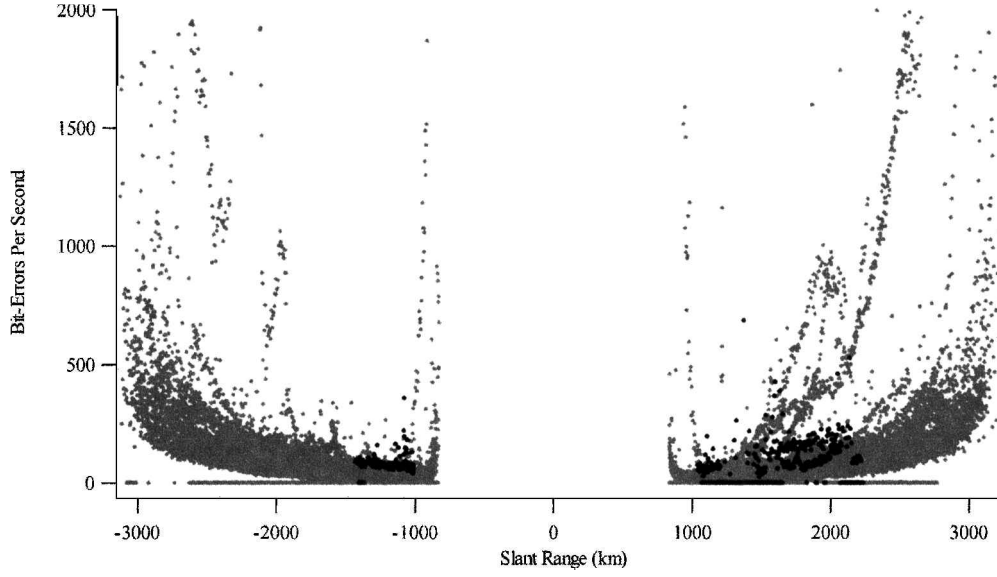

Fig. 4 Composite of all BER data for firings F-2, F-4, and F-7 (black dots) with all baseline data as a function of slant range from CPCA to ESEX (gray dots). The large increase near the center of the plot is a ground tracking phenomenon (keyhole) and is not indicative of a larger effect.

Table 2 Total velocity change, ΔV (m/s), during firings as measured by the accelerometer, ground tracking, and the GPS receiver

Firing	Accelerometer	Ground tracking	GPS
1	0.1089 ± 0.0207	0.11101 ± 0.00129	0.110 ± 0.003
2	0.2590 ± 0.0244	0.26023 ± 0.00129	N/A
3	0.2850 ± 0.0279	0.27304 ± 0.00129	N/A
4	0.4010 ± 0.0326	0.40348 ± 0.00129	N/A
5	0.3203 ± 0.0303	0.32809 ± 0.00129	N/A
6	0.2275 ± 0.0216	0.22699 ± 0.00129	N/A
7	0.0626 ± 0.0177	0.06563 ± 0.00129	N/A
8	0.0248 ± 0.0137	0.02924 ± 0.00129	N/A

analyses suggest the arcjet current telemetry was repeatedly reading approximately 6% high,[14] which would tend to lower the I_{sp} for a fixed specific power. Because this discrepancy could not be absolutely confirmed, however, the data presented in Fig. 5 are uncorrected for the higher power readings. Figure 5 does show, however, the mean of the performance corrected for the power discrepancy (shown as an open circle) as an illustration of the effect of the 6% difference.[14] In summary, the measured I_{sp} was 786.2 ± 43.0 s, the efficiency was 0.267 ± 0.021, and the thrust was 1.93 ± 0.06 N.

AFSCN tracking is typically used for spacecraft orbit determination in support of nominal satellite operations. For the ESEX mission, these data were also used to determine the performance of the thruster by comparing the orbit solutions before and after a firing. This technique provided an independent verification of the thruster performance by measuring the total ΔV imparted to the spacecraft. Table 2 summarizes the results of the eight firings derived from the ground tracking data and compares these with the data obtained from the accelerometer and the GPS receiver.

Because the GPS receiver experienced some difficulty on-orbit, limited data were acquired. These data only allowed a gross performance comparison, rather than time-resolved analysis of the thrust profile. As can be seen in Table 2, results agree well with the AFSCN tracking and the accelerometer where the three data sets are all available.

Contamination Measurements

An array of sensors was positioned at strategic locations around the ESEX diagnostic deck (see Fig. 1) to assess the contamination effects of the arcjet firings.[15–17] Mass deposition, which can impact satellite optical and thermal control surfaces, was measured using four TQCMs. Thermal flux from the arcjet firing was measured using four radiometers coated with S13-GLO, a common thermal surface material with low solar absorptivity and high emissivity. A sample Ga–As solar array segment was placed near the arcjet nozzle and used to determine the potential for plasma/solar array interactions or obscuration of the solar flux, which can have a deleterious impact on satellite power generation capability.

The TQCM sensors and electronics were powered on shortly after launch to characterize the vehicle outgassing and to provide a baseline to compare with other TQCM missions.[25] During these early operations, all of the sensors recorded deposition of material commensurate with spacecraft outgassing. Although no thermogravimetric analysis was performed to determine the specific constituents, typical effluents were expected because no special cleanliness requirements were levied on the spacecraft. During the subsequent eight firings of the ESEX arcjet, no measurable material deposition was observed on the TQCMs attributable to the steady-state operation of the arcjet. Material was collected on the sensor nearest the thruster exit plane (TQCM sensor 1) on the first firing; however, the lack of similar collection on subsequent firings or on any of the other sensors suggests this material was a one-time efflux indicative of the fabrication and handling and not indicative of steady-state contamination rates. TQCM sensor 2, which was not in the line of sight of the arcjet body or the plume, showed essentially no effect from the firings. Surprisingly, the TQCM sensors within the arcjet line of sight generally showed a removal of previously deposited mass with each firing, presumably as a result of heat flux from the arcjet causing vaporization of previously collected material.

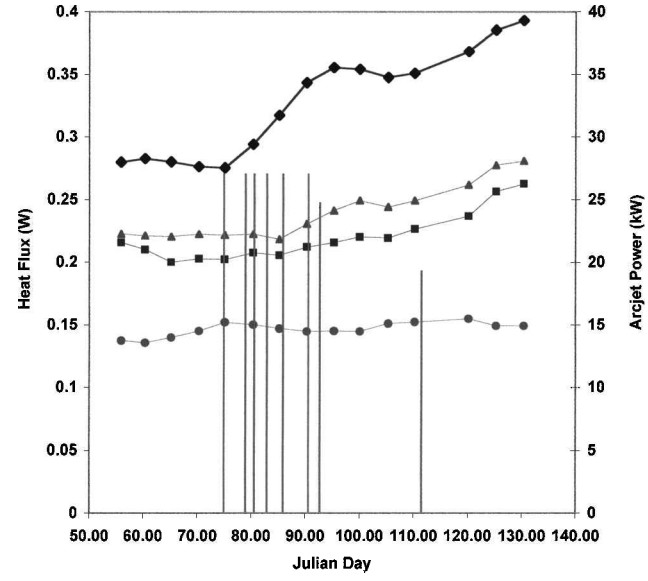

Fig. 6 Radiometer peak heat flux measurements during the ESEX firings. (The eight arcjet firings are indicated by the vertical lines.)

The radiometers are passive devices because they only require two temperature measurements, and so the data from these sensors were recorded throughout the ESEX mission. Measurement of the solar heat flux through the coating identified the degradation of the S13-GLO when subjected to the spectral emission of the high-power arcjet. This degradation is indicative of the effects on the thermal design of a spacecraft using high-power arcjets for propulsion. Figure 6 shows a summary of the maximum heat flux measured by the radiometers during the arcjet firing portion of the mission. In Fig. 6, the firings are indicated by vertical lines, with the corresponding arcjet power shown on the secondary axis. Radiometer 1, placed near the thruster exit with a view of both the arcjet plume and body, experienced an increase in the heat flux during the firings, indicating a degradation of the S13-GLO from the arcjet firings. The other radiometers, which had no view of the arcjet, or a view of only the plume, experienced less degradation as a result of the firings. There is also a noticeable increase in the heat flux on sensors 1, 2, and 4 as a result of the battery anomaly, which occurred on Julian day 114, presumably from the deposition of the battery effluents (this is corroborated by an increase in the mass deposition rates observed on the TQCMs).

Solar cell segments placed near the thruster exhaust recorded degradation in performance as well, observed as a temporary drop in open-circuit voltage, during the initial portion of the ramp-up phase of each firing and worsened as the mission progressed. This degradation was attributed to the arcjet exhaust plasma partially shorting the solar cell load. A summary plot of the solar cell voltage–current data is shown in Fig. 7 for the six full power firings (F-1C–F6, labeled Arcjet On), with comparable data for immediately after the arcjet was turned off, but while the arcjet body was still incandescent (labeled Arcjet Off). Whereas the data from the nonfiring cases fall on a single curve, the decrease in open circuit voltage observed when the arcjet was fired worsened with each firing, indicating a worsening effect. The decrease in solar cell open-circuit voltage was attributed to the plasma shorting the solar cell output through exposed leads on the cell. The worsening was attributed to degradation in these leads, possibly from erosion of the insulation, or sputtering of the surface, resulting in an increase in the surface area and more plasma contact with the leads. The solar array measurements also showed a 3% decrease in power generation over the 60-day period in which the arcjet was fired, which was attributed to degradation in the solar transmissivity of the cover glass material. No deleterious effects associated with the arcjet firings were observed on the main ARGOS solar arrays.

In general the ESEX results are very promising for the integration of high-power electric propulsion on commercial and government satellites. Although degradation associated with contamination was

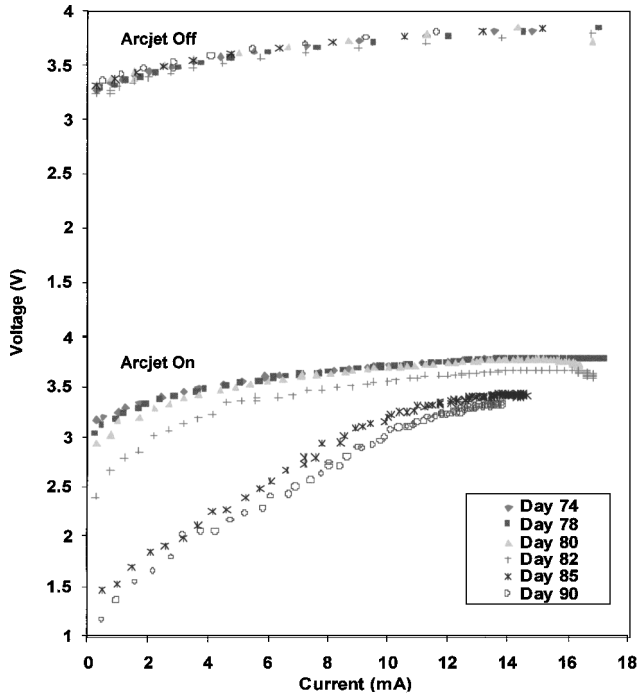

Fig. 7 Summary of the solar cell performance during the arcjet firings.

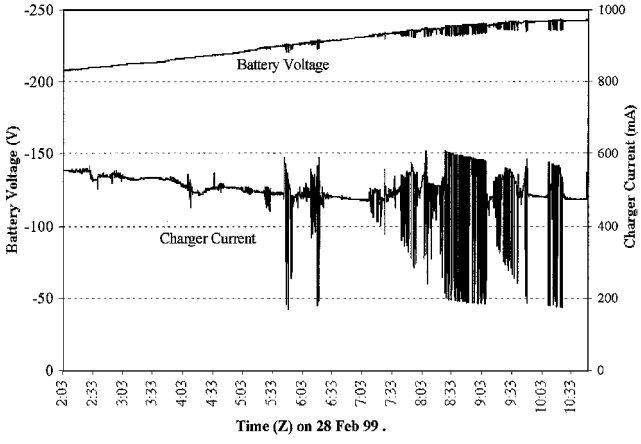

Fig. 8 Typical battery charging circuit instability.

observed, in each case the effect was manifested only on sensors placed near the exhaust nozzle. Sensitive materials or critical sensors would not likely be located as close to the arcjet exit plane in a fully developed, high-power electric propulsion system. Contamination sensors located in the backplane of the arcjet, or behind the thermal shield, showed no deleterious effects.

Flight Anomalies

The two anomalies to be discussed in detail are a battery failure that ultimately led to the conclusion of the ESEX mission and an observation of liquid ingestion in the PFS. The observed data are discussed, followed by a discussion of the proposed causes and resultant fixes, if applicable.

Battery Anomaly

The first signs of anomalous behavior in the battery were observed during the first charging cycle, shortly following the first ARGOS sunsafe event. The charging circuit operated nominally (except for a lower output current than expected) until the battery voltage approached −225 V dc. Once the battery attained this state of charge, as shown in Fig. 8, the output current from the charging circuit began cycling on and off, resulting in oscillations of the open-circuit battery voltage. These oscillations are believed to be a result of higher-than-expected internal battery impedance, perhaps exacerbated by a low-charging-circuit output current. In an attempt to lower the charging-circuit impedance, high-capacitance filters were switched into the circuit via high-voltage relays connecting the battery with the PCU.[7,8] Although this lower impedance decreased the frequency of the oscillations, it did not eliminate them entirely. Because this instability was not detrimental to the ESEX battery or the spacecraft bus, the charging continued through these oscillations, and the charging inefficiencies were accounted for by extending the total charging time. Subsequent charge cycles showed increasingly degraded stability that caused the charging circuit to shut off before attaining a full state of charge.

Beginning on F-4, further anomalous behavior on the battery output was observed, which resulted in limited firing duration. The battery output voltage dropped while firing the arcjet, resulting in unstable PCU and arcjet operation, and eventually extinguished the arc. Note, however, that the voltage at which the arc extinguished was less than −150 V dc, which was well below the lower PCU specification limit of −160 V dc. As can be seen in Table 1, the duration of each firing after F-4 steadily decreased, as the battery performance deteriorated. On F-7, the arcjet cycled on and off twice due to the command logic in the PCU, with both firings having extremely short durations. After this event, an attempt to recondition the battery was performed by executing a deep discharge through the battery bleed resistors[18] and restarting the charge. The initial plan was to wait until the battery was at a full state of charge (indicated by the charger circuit shutting off at the upper charge limit) before attempting the next firing. After 19 days passed without an automatic shutoff, the charger was commanded off, and a firing was attempted. Unfortunately, as can be seen by the short duration of F-8, the reconditioning did not have the desired effect.

Following the completion of F-8, the battery voltage fluctuated erratically between −175 and −200 V dc with periodic drops as low as −30 V dc, where it eventually stabilized. This behavior lasted approximately 24 h until, as subsequent analysis revealed, the battery subassembly on panel 1 (see Fig. 1) had a catastrophic failure. The failure was most likely a result of electrolyte leakage from one of the cells, causing a short circuit to the battery case. As the energy in the cell was discharging through the short circuit, there was a corresponding, dramatic increase in battery temperature, coupled with an increase in pressure as hydrogen gas was generated from decomposition of the electrolyte. This process continued until there was a breach of the battery case and a release of this super-heated gas internal to the ESEX flight unit. The gas was ultimately vented into space, causing a dramatic attitude disturbance on the vehicle, resulting in a sunsafe event. Spanjers et al.[15] include a discussion on the contamination effects from the battery venting.

An analysis of the failure was conducted[26]; however, the exact cause of the battery problem could not be fully determined because the flight data do not present a complete picture of the anomaly. There was, almost certainly, a combination of effects that ultimately describe the observed data set. Recent data show, for instance, a significant increase in the impedance of a Ag–Zn battery as it approaches a full state of charge at a low charge rate, which would explain the charger instabilities but not the ultimate failure. Some phenomenon was responsible for rupturing at least one of the battery cells and causing electrolyte to leak out and short to the battery case. It is also likely that some of the electrolyte was vented from the battery cells during launch as the flight unit depressurized and, also, as the high-current firings were conducted. This expelled electrolyte could have led to a variety of problems such as degraded mechanical connections or bridging the two cell electrodes and causing a short. In any case, this battery was pushed beyond its normal operating characteristics and was still able to deliver eight successful firings.

Several lessons were learned from the anomaly regarding the use of these batteries for this type of application.[26] In the initial design, the charging circuit was constrained by the amount of power available from the spacecraft. The design solution was to charge the battery at 0.67 A, rather than more typical values of 1–10 A. In hindsight, a better solution would have been to charge at the higher current to ensure traceability to previous applications but with a shorter duty cycle to satisfy orbit average power constraints. Another issue identified in the failure analyses was the encapsulation

of the battery cell interconnections in potting compound. Because these interconnections were subjected to the ESEX discharge currents (which were also higher than typical applications) and corresponding ohmic heating, the electrical characteristics between the cells and the interconnections could have been compromised. Again, in hindsight, a design that accommodated these high discharge rates might have avoided this failure. Finally, there was inadequate testing of the integrated battery and charging circuit before launch. Because of thermal constraints on the charging circuit in ambient conditions, all of the charging-circuit tests were limited in time to a few minutes rather than an entire charging cycle with the full battery assembly. A test of the system in the flight configuration, under orbital conditions, and conducted in the same operational way, would have identified the problem on the ground, with enough time to implement a solution before the flight.

As already mentioned, the battery failure occurred within days of the planned completion of phase II and, therefore, did not greatly affect the science data return. The primary result was a reduced number of firings observed from MSSS, which reduced the amount of arcjet firing spectra. Although this loss accounted for almost half of the missing mission data set (10% out of 24%), the impact to the overall mission success was small. In terms of the demonstration aspects of the mission, the battery was not critical because an operational system would be powered directly from the spacecraft power system. The critical demonstration components, the arcjet, PCU, and PFS, all operated successfully.

PFS Liquid Ingestion

The liquid ingestion was initially observed on the first successful ammonia outflow (R-3; Table 1). On initiation of the PFS algorithm, evidence of a single slug of liquid ammonia ingested into the plenum tank was observed on the initial DPC valve cycle. Figure 9 illustrates the issue for a typical outflow. (Note that the plenum tank pressure output saturates at 6.89×10^5 Pa.) As can be seen, the plenum tank temperature decreases by greater than 35°C within 30 s of initiating the PFS algorithm, indicating that liquid ammonia is expanding into the plenum tank. Approximately 5 min later, the plenum tank pressure and temperature indicate a superheated condition and drying out of the liquid in the plenum tank as some of the ammonia vapor is vented through the open arcjet valve (indicated in Fig. 9 by Begin outflow at 160 mg/s). A flow meter immersion thermistor located just upstream of the arcjet shows no corresponding drop in temperature, indicating that the liquid is confined to the plenum tank and never passed to the arcjet, even before arc initiation. To ensure that no two-phase flow reached the arcjet, however, the arcjet start was delayed until a dry plenum was achieved in all cases. After the initial ingestion, all PFS temperatures and pressures indicate no liquid was passed to the plenum tank or arcjet for any of the outflows or firings.

A schematic representation of the PFS is shown in Fig. 10. During operation,[6,18] the ammonia was stored in the propellant tank with the DPC valve closed until an arcjet firing. The system was heated to ensure sufficient pressure to support flow before a firing, the last 2 h of which included disabling the inlet heater on the propellant tank and enabling the heater on the plenum tank. This heater configuration vaporized some of the ammonia and drove that vapor to the propellant tank outlet to help ensure vapor-only flow to the arcjet. The enhanced feedline heater (EFH) was enabled to ready the system for the impending flow 7 min before a firing. The flow was initiated by enabling the PFS algorithm, which controlled the ammonia flow rate by cycling the DPC valve to maintain pressure in the plenum tank corresponding to the commanded flow rate. As a result of the software encoding, however, the DPC valve cycled once at the start of the PFS algorithm regardless of the plenum tank pressure. Finally, the arcjet valve was opened, and the flow to the arcjet was monitored through the sonic venturi flow meter.

PFS heater performance before the outflow indicated that the bulk of the ammonia liquid remained away from the outlet of the propellant tank as the design intended. As already described, keeping the liquid ammonia away from the tank outlet was accomplished by differential heating of the propellant tank poles, but was also possibly aided by the angular momentum of the spacecraft in orbit. During the outflow, and throughout the mission, temperatures of the EFH indicated relatively little liquid entering the EFH and 100% vapor outflow at the exit.

The liquid ingestion phenomenon was not readily observed in any of the ground tests. Initially, there were some minor differences between heater setpoints and timing of the flight operations profile and the ground tests as a result of the final thermal analyses

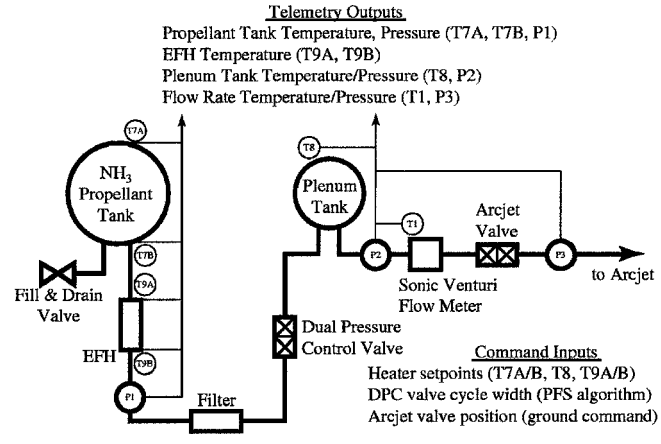

Fig. 10 Schematic representation of the PFS.

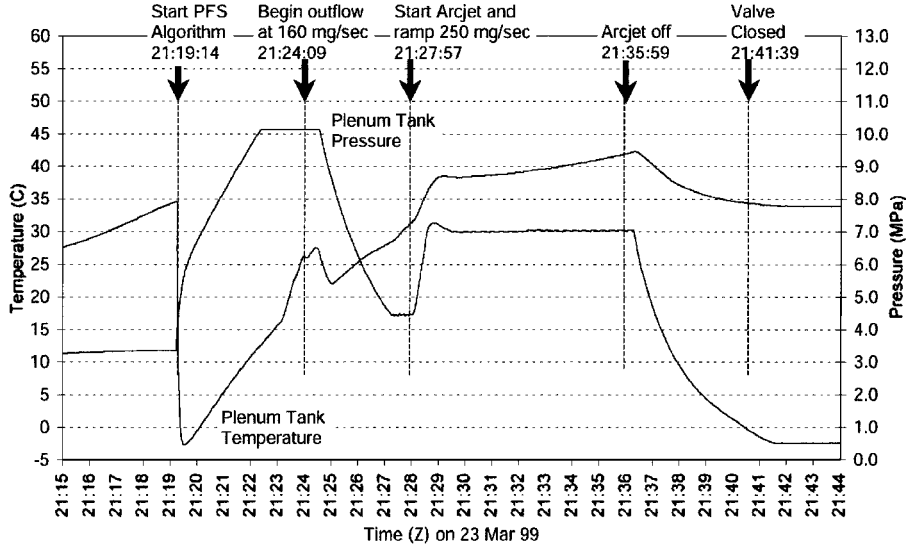

Fig. 9 Typical PFS performance showing liquid ingestion into the plenum tank.

conducted before the PFS integration. During the course of the on-orbit troubleshooting, the flight profile was changed back to mirror the test flow in an attempt to link the operational use with the test experiences, but the revised profile did not alleviate the problem.

Further troubleshooting identified a potential thermal gradient in the section of tubing between the EFH and the DPC valve, which could allow the ammonia to pool just upstream of the valve and result in the ingestion of a large slug of liquid. Thermal modeling of this region was performed to attempt to identify an operational profile that would eliminate the temperature gradient, and more heater setpoint modifications were made to the flight profile. Largely due to the lack of direct thermal control of this section of tubing, however, none of these changes proved successful.

The liquid ingestion appeared to be the result of a cold section of the propellant line, likely a result of a cooler mounting platform than experienced during test, coupled with the thermal gradient between the EFH and the DPC valve. The platform temperature is not actively controlled, and the thermal analyses showed it could drift significantly low enough to condense ammonia at the pressure in the propellant line just upstream of the DPC valve. As already described, every time the PFS algorithm is initiated, the DPC valve is cycled once, which released a slug of liquefied ammonia into the plenum tank. These data are supported by the fact that liquid ingestion was never observed during any steady-state operations of the PFS. To further support this hypothesis, there were some variations from the normal procedure on the last firing (F-8), and no liquid ingestion was observed. For this firing, the PFS heaters were turned on several days before the firing attempt while waiting for the battery reconditioning to complete, which increased the overall flight unit temperature 6–12°C and eliminated the cold spot in the propellant line.

In summary, the liquid ingestion proved to be an annoyance, but did not seriously detract from the arcjet operation. If the ESEX mission had continued, a heater configuration that alleviated the problem would almost certainly have been identified. Other than this issue, the PFS performed within specification and, in general, operated exceptionally well. The flow rate control generally operated to within ±0.3 mg/s at steady-state conditions, which was more than an order of magnitude better than the requirement of ±5 mg/s. If the flow system evolved into an operational flight design, some heater power applied to the section of the propellant line in question, or more direct thermal control of that section, could almost certainly resolve the liquid ingestion issue entirely, especially in light of the results from the last firing.

Conclusions

ESEX is the culmination of over 10 years of effort to validate high-power electric propulsion on-orbit and verify the compatibility with standard U.S. Air Force satellites. There were a total of eight firings conducted over the course of the 60-day mission, for a total duration of 2023 s. There were two anomalies associated with the flight operations: a liquid ammonia ingestion problem that had only a minor affect on the mission and a battery failure that precluded any further firings. Approximately 76% of the ESEX mission success was attained, with the biggest deficiencies resulting from the lack of a complete optical signature characterization and the lack of GPS data. All of the demonstration aspects of the experiment were completed, and all of the demonstration hardware, the arcjet, PCU, and PFS, operated well and within their specifications. The ESEX flight demonstrated high-power electric propulsion is compatible with satellite operations. All data show the thruster and the high-power components have no significant, deleterious effect on any satellite activities.

Acknowledgments

The authors would like to extend their gratitude to the U.S. Air Force Research Laboratory support team including Jim Zimmerman, Dwayne Matias, Scott Engelman, Alan Sutton, Bill Hargus, Ron Spores, Shaughn Tracy, Krystin Barker, Rickie Rexroade, and Robin Lowder. We also extend our thanks to Mary Kriebel, Don Baxter, David Lee, David Huang, and Bob Tobias of TRW, Inc., for their technical expertise on the Electric Propulsion Space Experiment (ESEX) flight hardware, and to Andy Hoskins, Joe Cassady, Bob Kay, and David King of Primex Aerospace Company for their technical insight into the arcjet, propellant feed system, and power conditioning unit. We would also like to extend our sincere gratitude to the ARGOS program office and the entire flight operations team at Kirtland Air Force Base, New Mexico, as well as the staff at the Maui Space Surveillance Site and the Camp Parks Communications Annex for their technical expertise, as well as their insight into and flexibility with their facilities. This out-of-the-box mentality allowed ESEX to acquire such a broad range of data.

References

[1]Kriebel, M. M., and Stevens, N. J., "30-kW Class Arcjet Advanced Technology Transition Demonstration (ATTD) Flight Experiment Diagnostic Package," AIAA Paper 92-3561, July 1992.

[2]Sutton, A. M., Bromaghim, D. R., and Johnson, L. K., "Electric Propulsion Space Experiment (ESEX) Flight Qualification and Operations," AIAA Paper 95-2503, July 1995.

[3]LeDuc, J. R., McFall, K. M., Tilley, D. L., Sutton, A. M., Pobst, J. A., Bromaghim, D. R., and Johnson, L. K., "Performance, Contamination, Electromagnetic, and Optical Flight Measurement Development for the Electric Propulsion Space Experiment," AIAA Paper 96-2727, July 1996.

[4]Turner, B. J., and Agardy, F. J., "The Advanced Research and Global Observation Satellite (ARGOS) Program," AIAA Paper 94-4580, Sept. 1994.

[5]Agardy, F. J., and Cleave, R. R., "A Strategy for Maximizing the Scientific Return Using a Multi-Phased Mission Design for ARGOS," American Astronautical Society, AAS Paper 93-594, Aug. 1993.

[6]Vaughan, C. E., and Morris, J. P., "Propellant Feed Subsystem for a 26 kW Flight Arcjet Propulsion System," AIAA Paper 93-2400, June 1993.

[7]Biess, J. J., and Sutton, A. M., "Integration and Verification of a 30 kW Arcjet Spacecraft System," AIAA Paper 94-3143, June 1994.

[8]Vaughan, C. E., Cassady, R. J., and Fisher, J. R., "Design, Fabrication, and Test of a 26 kW Arcjet and Power Conditioning Unit," International Electric Propulsion Conf., IEPC Paper 93-048, Sept. 1993.

[9]Cassady, R. J., Hoskins, W. A., Vaughan, C. E., Aadland, R. S., Morris, J. P., Kay, R. J., and Fisher, J. R., "The Development and Flight Qualification of a 26 kW Arcjet Propulsion Subsystem," *Journal of Propulsion and Power*, Special Issue on Electric Propulsion Space Experiment (ESEX) flight (submitted for publication).

[10]Kriebel, M. M., "System Engineering, Design, Integration and Qualification of the Electric Propulsion Space Experiment Flight Unit," *Journal of Propulsion and Power*, Special Issue on Electric Propulsion Space Experiment (ESEX) flight (submitted for publication); also AFRL-PR-ED-TR-1999-0034, 1999.

[11]Bromaghim, D. R., LeDuc, J. R., Salasovich, R. M., and Johnson, L. K., "A Review of the Electric Propulsion Space Experiment Program," *Journal of Propulsion and Power*, Special Issue on Electric Propulsion Space Experiment (ESEX) flight (submitted for publication).

[12]Johnson, L. K., Spanjers, G. G., Bromaghim, D. R., and Dulligan, M. J., "On-Orbit Optical Observations of ESEX 26 kW Ammonia Arcjet," *Journal of Propulsion and Power*, Special Issue on Electric Propulsion Space Experiment (ESEX) flight (submitted for publication); also AIAA Paper 99-2710, June 1999.

[13]Dulligan, M. J., Zimmerman, J. A., Salasovich, R. M., Bromaghim, D. R., and Johnson, L. K., "Observations of the Effects on Spacecraft Function and Communications by the ESEX 26 kW Ammonia Arcjet Operations," *Journal of Propulsion and Power*, Special Issue on Electric Propulsion Space Experiment (ESEX) flight (submitted for publication); also AIAA Paper 99-2708, June 1999.

[14]Fife, J. M., Bromaghim, D. R., Chart, D., Hoskins, W. A., Vaughan, C. E., and Johnson, L. K., "Refined Orbital Performance Measurements of the Air Force Electric Propulsion Space Experiment (ESEX) Ammonia Arcjet," *Journal of Propulsion and Power*, Special Issue on Electric Propulsion Space Experiment (ESEX) flight (submitted for publication); also AIAA Paper 99-2707, 1999.

[15]Spanjers, G. G., Schilling, J. H., Engelman, S. F., Bromaghim, D. R., and Johnson, L. K., "Mass Deposition Measurements from the 26-kW Electric Propulsion Space Experiment Flight," *Journal of Propulsion and Power*, Special Issue on Electric Propulsion Space Experiment (ESEX) flight (submitted for publication); also International Electric Propulsion Conf., IEPC Paper 99-038, Oct. 1999.

[16]Schilling, J. H., Spanjers, G. G., Bromaghim, D. R., and Johnson, L. K., "Solar Cell Degradation during the 26-kW Electric Propulsion Space Experiment Flight," *Journal of Propulsion and Power*, Special Issue on Electric Propulsion Space Experiment (ESEX) flight (submitted for publication); also International Electric Propulsion Conf., IEPC Paper 99-038, Oct. 1999.

[17]Spanjers, G. G., Schilling, J. H., Engelman, S. F., Bromaghim, D. R., and Johnson, L. K., "Radiometric Analysis from the 26-kW Electric Propulsion

Space Experiment Flight," *Journal of Propulsion and Power*, Special Issue on Electric Propulsion Space Experiment (ESEX) flight (submitted for publication); also International Electric Propulsion Conf., IEPC Paper 99-038, Oct. 1999.

[18]Bromaghim, D. R., and Sutton, A. M., "Electric Propulsion Space Experiment Integration and Test Activities on the Advanced Research and Global Observation Satellite," AIAA Paper 96-2726, July 1996.

[19]Salasovich, R. M., Bromaghim, D. R., and Johnson, L. K., "Diagnostics and Flight Planning for the U.S. Air Force Phillips Laboratory Electric Propulsion Space Experiment," AIAA Paper 97-2777, July 1999.

[20]Aadland, R. S., Vaughan, C. E., Hoskins, W. A., and Kay, R. J., "Achieving Reliable, Repeatable Starts of a 26 kW Arcjet" International Electric Propulsion Conf., IEPC Paper 93-049, Sept. 1993.

[21]Tilley, D. L., McFall, K. A., Castillo, S., Andrews, J. C., and Bromaghim, D. R., "An Investigation of the Breakdown Characteristics of a 30 kW Class Ammonia Arcjet," AIAA Paper 93-1901, June 1993.

[22]Tilley, D. L., "Propellant Breakdown Mechanisms in an Arcjet," International Electric Propulsion Conf., IEPC Paper 93-050, Sept. 1993.

[23]Johnson, L. K., Rivera, A., Lundquist, M., Sanks, T. M., Sutton, A. M., and Bromaghim, D. R., "Frequency-Domain Electromagnetic Characteristics of a 26 kW Ammonia Arcjet," *Journal of Spacecraft and Rockets*, Vol. 33, No. 1, 1996, pp. 137–143; also AIAA Paper 93-2393, June 1993.

[24]Cassady, R. J., Lichon, P. G., and King, D. Q., "Arcjet Endurance Test Program Final Report," U.S. Air Force Astronautics Lab., AL-TR-90-069, March 1991; also AIAA Paper 90-2532, July 1990.

[25]Wood, B. E., Hall, D. F., Lesho, J. C., Uy, O. M., Dyer, J. S., and Bernard, W. T., "MSX Satellite Flight Measurements of Contamination Deposition on a CQCM and on TQCMs," AIAA Paper 97-0841, Jan. 1997.

[26]Bromaghim, D. R., "Battery Failure on the Electric Propulsion Space Experiment (ESEX)," High Accident Potential (HAP) Rept., U.S. Air Force Space and Missile Systems Center; also U.S. Air Force Research Lab., AFRL-PR-ED-TR-2001-0027, 2001.

J. A. Martin
Associate Editor